RESEARCH ARTICLE

Vasorin plays a critical role in vascular smooth muscle cells and arterial functions

Loïc Louvet[1] | Gaëlle Lenglet[1] | A. Michaela Krautzberger[2] |
Romuald Mentaverri[1,3] | Frédéric Hague[4] | Clara Kowalewski[1] |
Nassim Mahtal[5] | Julie Lesieur[6] | Anne-Laure Bonnet[6,7] | Caroline Andrique[6] |
Céline Gaucher[6,7] | Cathy Gomila[1] | Heinrich Schrewe[2] | Pierre-Louis Tharaux[5] |
Said Kamel[1,3] | Catherine Chaussain[6,7] | Isabelle Six[1]

[1]UR 7517 UPJV, Pathophysiological Mechanisms and Consequences of Cardiovascular Calcifications (MP3CV), Picardie Jules Verne University, Amiens, France

[2]Department of Developmental Genetics, Max Planck Institute for Molecular Genetics, Berlin, Germany

[3]Amiens University Hospital, Human Biology Center, Amiens, France

[4]UR EA4667, UPJV, Laboratoire de Physiologie Cellulaire et Moléculaire, Picardie Jules Verne University, Amiens, France

[5]Université Paris Cité, Paris Cardiovascular Center, INSERM, Paris, France

[6]Université Paris Cité, URP2496, F-92120, Montrouge, France

[7]AP-HP, FHU DDS-net, Services de médecine bucco-dentaire (GH Sorbonne Université, GH Paris Nord Université de Paris, GH Henri Mondor), Paris, France

Correspondence
Isabelle Six, UR 7517 UPJV, Pathophysiological Mechanisms and Consequences of Cardiovascular Calcifications (MP3CV), Picardie Jules Verne University, 1 rue des Louvels, 80037 Amiens, France.
Email: isabelle.six@u-picardie.fr

Abstract

Within the cardiovascular system, the protein vasorin (Vasn) is predominantly expressed by vascular smooth muscle cells (VSMCs) in the coronary arteries and the aorta. *Vasn* knockout ($Vasn^{-/-}$) mice die within 3 weeks of birth. In the present study, we investigated the role of vascular Vasn expression on vascular function. We used inducible *Vasn* knockout mice ($Vasn^{CRE-ERT\ KO}$ and $Vasn^{SMMHC-CRE-ERT2\ KO}$, in which respectively all cells or SMCs only are targeted) to analyze the consequences of total or selective Vasn loss on vascular function. Furthermore, in vivo effects were investigated in vitro using human VSMCs. The death of $Vasn^{CRE-ERT\ KO}$ mice 21 days after tamoxifen injection was concomitant with decreases in blood pressure, angiotensin II levels, and vessel contractibility to phenylephrine. The $Vasn^{SMMHC-CRE-ERT2\ KO}$ mice displayed concomitant changes in vessel contractibility in response to phenylephrine and angiotensin II levels. In vitro, *VASN* deficiency was associated with a shift toward the SMC contractile phenotype, an increase in basal intracellular Ca^{2+} levels, and a decrease in the SMCs' ability to generate a calcium signal in response to carbachol or phenylephrine. Additionally, impaired endothelium-dependent relaxation (due to changes in nitric oxide signaling) was observed in all *Vasn* knockout mice models. Our present findings highlight the role played by Vasn SMC expression in the maintenance of vascular functions. The mechanistic experiments suggested that these effects are mediated by SMC phenotype switching and changes in intracellular calcium homeostasis, angiotensin II levels, and NO signaling.

KEYWORDS

angiotensin II, artery, nitric oxide, smooth muscle cells, vascular function, vasorin

---

Loïc Louvet and Gaëlle Lenglet contributed equally to this study.

---

1 | INTRODUCTION

Vasorin (Vasn) is a. type I transmembrane glycoprotein also known as SLIT-like 2. In humans and other animals, the protein is expressed in many tissues, organs, and biological fluids from the embryonic stage through to the adult stage (Bonnet et al., 2018; Krautzberger et al., 2012). In the cardiovascular system, Vasn is expressed in coronary arteries and in the aorta. At the vascular level, Vasn was detected both in vascular smooth muscle cells (VSMCs; Ikeda et al., 2004) and endothelial cells (ECs; Huang et al., 2015). Three forms of VASN have been identified: a transmembrane form (Ikeda et al., 2004; whose biological role has yet to be determined), an extracellular (secreted) form (Ikeda et al., 2004; Li et al., 2018; Malapeira et al., 2011; Man et al., 2018), and an intracellular form (also referred to as ATIA for Anti TNF-α Induced Apoptosis; Choksi et al., 2011). The signaling pathway associated with the secreted form of VASN is linked to the transforming growth factor-beta (TGF-β) pathway. The secreted form of VASN is able to inhibit TGF-β's binding to its receptors and thus blocks activation of the corresponding signaling partners (Ikeda et al., 2004). In a mouse model of restenosis, it has been shown that *Vasn* expression is downregulated during vessel repair after arterial injury. Experiments with adenovirus-mediated in vivo gene transfer in the same model have shown that *Vasn* overexpression in carotid arteries significantly decreases the formation of injury-induced vascular lesions. Moreover, *Vasn* downregulation was found to be associated with a proliferative/synthetic dedifferentiated phenotype that was associated with TGF-β-driven fibroproliferative response to vascular injury (Ikeda et al., 2004).

Pintus et al. recently evidenced a link between VASN, TGF-β, and angiotensin (Ang) II in aging arterial wall cells and in VSMCs. *Vasn* expression was downregulated and Ang II abundance was upregulated in aged animals through undeciphered mechanisms. Though, Ang II's stimulation of the AT1 receptor activated MMP-2, which increased VASN degradation and thus TGF-β activity (Pintus et al., 2018).

VASN's functions have not yet been unambiguously determined. However, the death of *Vasn* knockout (KO) mice (*Vasn*$^{-/-}$) mice around Day 21 after birth (Bonnet et al., 2018) shows clearly that the protein has critical roles in physiology. The objective of the present study was to assess the consequences of total or SMC-selective *Vasn* KO on mortality, vascular function, and blood pressure in adult mice.

2 | MATERIALS AND METHODS

Experimental procedures are further detailed in an extended section in the Supporting Information.

2.1 | Animals

Experiments were conducted according to the French legislation (Directive 2010/63/EU of the European Parliament) and the protocols were approved by the local Institution's Animal Care and Use Committee (APAFIS#13153-2018012310506063v2 for *Vasn*$^{CRE-ERT\ KO}$ mice and *Vasn*$^{SMMHC-CRE-ERT2\ KO}$ mic and APAF IS#25490-2019062016505841v4 for *Vasn*^{Venus} mice).

Age-matched C57BL/6J mice were used as controls.

We used *Vasn*$^{flox/flox}$ × CAGG-Cre-ER™ (Jackson Laboratory, #004682) mice to generate male or female *Vasn*$^{CRE-ERT\ KO}$ mice with conditional *Vasn* knockdown in all tissues. Male *Vasn*$^{SMMHC-CRE-ERT2\ KO}$ mice (with the conditional knockdown of *Vasn* in SMCs specifically) were obtained by crossing *Vasn*$^{flox/flox}$ × *Myh11*-Cre-ER^{T2} mice (Jackson Laboratory, #019079). At the age of 8 weeks, the mice received consecutive daily intraperitoneal injections of tamoxifen (1 mg/25 g of body weight) for 3 days. A group of aged *Vasn*$^{CRE-ERT\ KO}$ mice was obtained by injecting 1-year-old mice with tamoxifen.

Mortality was recorded daily in all the groups of mice.

Fourteen days and 21 days after tamoxifen injection of the *Vasn*$^{CRE-ERT\ KO}$ and *Vasn*$^{SMMHC-CRE-ERT2\ KO}$ mice, and 21 days after tamoxifen injection of the aged *Vasn*$^{CRE-ERT\ KO}$ mice, we measured the heart rate and the systolic, diastolic and mean arterial blood pressures using a noninvasive system (CODA®, Kent Scientific Corporation).

In a second step, 14 and 21 days after tamoxifen injection of the *Vasn*$^{CRE-ERT\ KO}$ and *Vasn*$^{SMMHC-CRE-ERT2\ KO}$ mice, they were anesthetized by injection with sodium pentobarbital (150 mg/kg) and blood samples were collected by cardiac puncture. Serum urea, phosphorus, and total calcium concentrations were measured using a Randox Daytona$^+$ autoanalyzer (Randox Global Healthcare). Serum endothelin 1 concentrations were measured by ELISA (Enzo Life Sciences, ADI-900-020A). Serum Ang II and asymmetric dimethylarginine (ADMA) concentrations were measured using competitive ELISAs (ADI-900-204 from Enzo Life Sciences and E-EL-0042 from Elab Sciences, respectively).

2.2 | Analysis of vessel Vasn expression pattern

To analyze vascular Vasn expression, we used the *Vasn*^{Venus} mice, which express the fluorescent protein Venus according to *Vasn* expression pattern. Aortas from *Vasn*^{Venus} reporter mice were included in paraffin and cut into 3 μm sections. Sections were co-stained with an anti-GFP antibody that bound to the Venus protein (ab290, Abcam; dilution: 1:1000) and with an anti-CD31 (DIA-310, Dianova GmbH; dilution: 1:200).

Some of the *Vasn*$^{CRE-ERT\ KO}$ mice and *Vasn*$^{SMMHC-CRE-ERT2\ KO}$ mice were used to analyze vascular reactivity, and the others were used to analyze RNA and protein expression in vessels.

For histological analyses, aortas were included in optimal cutting temperature compound and subsequently cut into 4 μm sections. For each vessel ring, 10 nonconsecutive round-shaped sections were selected at random and stained with hematoxylin (*n* = 5 per ring) or immunostained for Vasn detection (*n* = 5 per ring). For the quantification of Vasn in ECs and VSMCs, the intensity of Vasn staining on each section was graded from 0 to 4.

Endothelial immunostaining was performed using the same method (anti-CD31, 1:25 dilution, Ab182981, Abcam; Maizel

et al., 2009) to confirm the presence of ECs at the luminal surface of the vessel wall.

Vasn was also immunoblotted with a rabbit anti-Vasn antibody (1:250 dilution in TBST/milk, home-made antibody, Max Planck Institute for Molecular Genetics).

For qPCR analyses, tissue samples were disrupted in TRI reagent (Sigma-Aldrich), using a Bio-Gen PRO 200 homogenizer (PRO Scientific Inc). Depending on the amount of the tissue, RNA was extracted using an RNeasy Plus Mini Kit or an RNeasy Plus Micro Kit (Qiagen).

2.3 | Involvement of Vasn in arterial function

At the experimental endpoint, the animals were anesthetized by injection of sodium pentobarbital (150 mg/kg) and euthanasia was accomplished by the removal of the heart in accordance with French legislation. The descending thoracic aorta (for use in vascular responsiveness experiments) was then carefully removed, as reported previously (Maizel et al., 2009).

Each aorta used for vascular reactivity was sectioned into 3.5 mm rings devoid of fat and connective tissue and vascular reactivity studies were carried out as previously described (Maizel et al., 2009).

2.4 | *VASN* silencing in human vascular smooth muscle cells and human umbilical vein endothelial cells in culture

Human vascular smooth muscle cells (HVSMCs) were isolated from aortic tissue using an explant technique. The aortic tissue samples were obtained from patients with a mean age of 64 ± 4 years in accordance with French legislation (reference: PI 2021_843_0002). Our experiments with human cells complied with the principles outlined in the Declaration of Helsinki. The experimental cell model of HVSMCs is a well-established model routinely used in our laboratory (Louvet et al., 2013; Six et al., 2014). The HVSMCs were used between passages 4 and 6. Human umbilical vein endothelial cells (HUVECs; C-12203; PromoCell) were cultured in EC Growth Medium-2 (C-22011; PromoCell) supplemented with EGM-2 Supplement Mix containing EC growth complement (C-39216; Promo-Cell). The EGM-2 medium was changed every 2 days and cells were used between passages 2 and 4, except as indicated.

Using siPORTNeoFX technology (1013004; Thermo Fisher Scientific), we transfected HVSMCs or HUVECs for 72 h with either two small interfering RNAs (siRNAs) against *VASN* mRNA (siVasn; s41740 and s41741; Ambion®) or a nontargeting siRNA (a negative control, siNeg; AM4636; Ambion®).

2.5 | Impact of *VASN* silencing on HVSMC phenotypes

We evaluated the impact of *VASN* silencing on HVSMC phenotypes by assessing the expression of genes associated with a contractile phenotype (CNN1, α-SMA, and SMMHC) and those associated with the synthetic phenotype (Coll8, Coll1, and OPN; Supporting Information: Table 1). RNA isolation, reverse transcription, and real-time quantitative PCR (qPCR) are detailed in the Supporting Information.

2.6 | The influence of VASN on the HVSMCs' intracellular calcium content

After transfection, cells were loaded for 1 h with Fura-2/acetoxymethyl (Fura 2/AM, 3 μM in medium) as described previously (Daya et al., 2021). HVSMCs were stimulated with the muscarinic agonist carbachol (10 μM) or the selective α1-adrenergic agonist phenylephrine. Both compounds raise the intracellular calcium level ($[Ca^{2+}]_i$) and thus cause the SMCs to contract.

To measure divalent cation influx, we used an Mn^{2+} quenching protocol.

The expression of the specifically stimulated metabotropic receptors was also assessed in HVSMCs (Supporting Information: Table 2).

2.7 | *Vasn* deletion in the aorta and consecutive changes in signaling pathways

Proteins from aorta samples were extracted with RIPA buffer supplemented with a proteinase inhibitor cocktail, PMSF and vanadate. The protein content of each lysate sample was determined using the DC™ protein assay kit (Bio-Rad). The whole Western blot procedures and used antibodies are detailed in the relative Supporting Information.

We evaluated the impact of *Vasn* silencing on STAT3 expression and VSMC phenotype switching by probing samples with antibodies against total STAT3 (t-STAT3) and phospho- STAT3 (p-STAT3).

The status of the contraction signaling pathway was investigated by using antibodies against phospho-MYPT1 (p-MYPT1) and the AT1 receptor.

The status of the relaxation signaling pathway was investigated by using antibodies against total-AKT (t-AKT), phospho-AKT (p-AKT), total-eNOS (t-eNOS), and phospho-eNOS (p-eNOS).

Immunoblot images were acquired and quantified using Chemi-Doc software (Bio-Rad) and ImageJ software (NIH).

2.8 | The influence of *VASN* deletion in HUVECs on the NO pathway

VASN mRNA and protein expressions were assessed for passages P2–P6 of the HUVECs culture in *VASN*-silenced HUVECs. HUVECs viability was tested using the classical MTT assay. The relaxation signaling pathway was investigated in HUVECs using antibodies against t-eNOS and p-eNOS. NO production by HUVECs was

assessed by measuring the fluorescence of 4-amino-5-methylamino-2′,7′-difluorescein diacetate (DAF-FM DA), a specific NO probe, in microplates. After overnight serum starvation, HUVECs microplates were loaded with DAF-FM DA (1 μM) for 30 min. Fluorescence was measured after washing and incubation using a spectrofluorometer (TECAN Spark), with an excitation wavelength of 505 nm and an emission wavelength of 530 nm. Inhibition of NO production by eNOS using the inhibitor N-nitro-L-arginine methyl ester (L-NAME, 100 μM) was also included in the experiments.

2.9 | Statistical analysis

Data are presented as means ± SEM. For non-parametric data, Kruskal–Wallis test was used to determine significant differences in means between all groups (if groups were > 2), followed by Mann–Whitney U-test to compare to seek the significance of differences between 2 groups. For parametric data, when more than two means were compared, analysis of variance with or without repeated measurements (ANOVA) was used. If a significant overall difference was found, Bonferroni's test was used to identify differences between groups. The strength of the association between Ang II levels and contractions in response to phenylephrine was determined by calculating Pearson's correlation coefficient. The threshold for statistical significance was set to $p < 0.05$.

3 | RESULTS

Vessels from $Vasn^{-/-}$ mice did not contract in response to potassium or phenylephrine. Direct addition of acetylcholine to the organ chamber induced weak relaxation that could not be quantified because of the lack of contraction beforehand. The $Vasn^{-/-}$ mouse model was challenging to use (given the very small vessel size, due to the mice's young age), and so the observed vascular dysfunction could not be adequately characterized. Accordingly, we then developed the $Vasn^{CRE-ERT}$ ^{KO} model for assessment of the effect of $Vasn$ deletion in adult mice.

3.1 | Elevated mortality at 21 days is observed in $Vasn^{CRE-ERT}$ ^{KO} mice but not in $Vasn^{SMMHC-CRE-ERT2}$ ^{KO} mice

In $Vasn^{CRE-ERT}$ ^{KO} mice, the deletion of $Vasn$ in all tissues had no effect on biological parameters measured 14 days after CRE induction. However, 21 days after induction, these mice displayed an elevated body weight ($p < 0.01$ vs. control mice). No other changes in biological parameters were observed in $Vasn^{SMMHC-CRE-ERT2}$ ^{KO} mice 14- and 21-day post-induction (Supporting Information: Table 3).

Twenty-one days after the injection of tamoxifen, we observed elevated mortality among $Vasn^{CRE-ERT}$ ^{KO} mice but not among $Vasn^{SMMHC-CRE-ERT2}$ ^{KO} mice. None of the 26 mice that did not receive tamoxifen died, whereas 9 of the 46 (20%) tamoxifen-treated $Vasn^{CRE-ERT}$ ^{KO} mice were found dead shortly before the end of the study program at 21 days after $Vasn$ deletion induction.

3.2 | Modulation of vascular Vasn expression in animal models

The results of experiments on $Vasn^{Venus}$ transgenic mice suggested that the $Vasn$ gene was expressed in ECs and SMCs from the thoracic aorta (Figure 1a).

In $Vasn^{CRE-ERT}$ ^{KO} mice, the level of $Vasn$ mRNA was significantly lower in the thoracic aorta (by 80%), heart, kidney, and lung (all $p < 0.01$ vs. control mice). In the aorta, the decrease in $Vasn$ mRNA was associated with a significant decrease in Vasn protein (−90%, $p < 0.05$ vs. control mice) and deletion was confirmed by a reduced Vasn labeling both in ECs (−75%, $p < 0.001$ vs. controls) and in SMCs (−54%, $p < 0.001$ vs. controls) from $Vasn^{CRE-ERT}$ ^{KO} mice (Figure 1b).

In tamoxifen-injected $Vasn^{SMMHC-CRE-ERT2}$ ^{KO} mice, we observed low levels of $Vasn$ mRNA expression (−65%, $p < 0.05$ vs. control mice) and Vasn protein expression (−86%, $p < 0.05$ vs. control mice) in the thoracic aorta samples only. Vasn labeling was deleted only in the tunica media (−57%, $p < 0.001$ vs. controls) of $Vasn^{SMMHC-CRE-ERT2}$ ^{KO} mice (Figure 1c). To complete our investigation of the potential effect of $Vasn$ deletion on the vessel wall in $Vasn^{SMMHC-CRE-ERT2}$ ^{KO} mice, CD31 immunostaining showed that the endothelium was present.

3.3 | Effect of Vasn deletion on systolic, diastolic, and mean blood pressure values, heart rate, endothelin 1, and Ang II levels
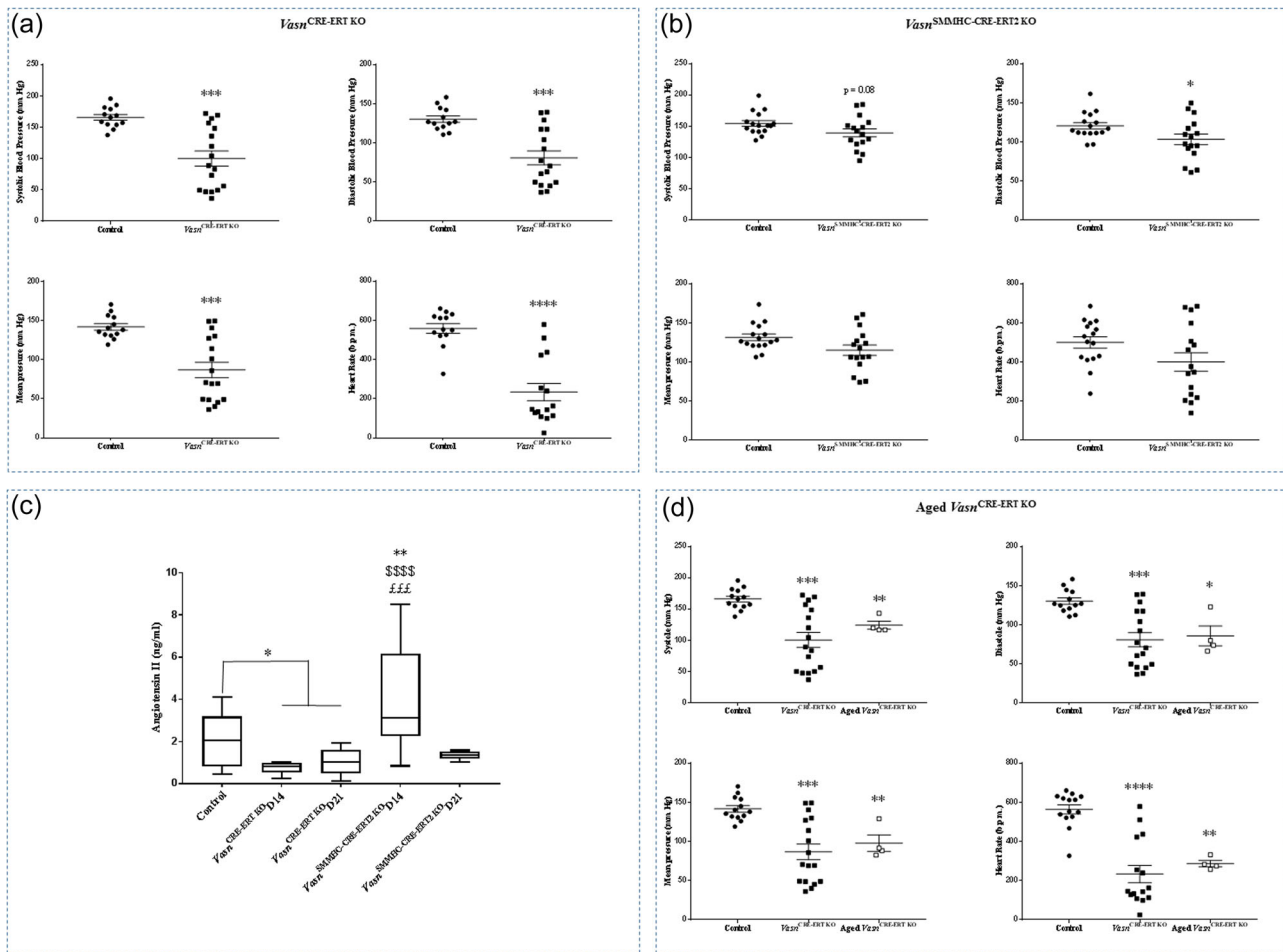
$Vasn^{CRE-ERT}$ ^{KO} mice displayed significantly lower systolic, diastolic, and mean arterial blood pressure and heart rate 21 days after tamoxifen injection ($p < 0.0005$ vs. control mice, Figure 2a). The same pattern was observed for $Vasn^{SMMHC-CRE-ERT2}$ ^{KO} mice and was statistically significant for decreased diastolic blood pressure relative to control mice ($p < 0.05$, Figure 2b).

However, the measure of Ang II levels at 14 and 21 days were significantly ($p < 0.05$) lower in $Vasn^{CRE-ERT}$ ^{KO} mice (0.74 ± 0.12 and 1.03 ± 0.20 ng/ml, respectively) than in controls (2.06 ± 0.36; Figure 2c). In contrast, the serum Ang II level was found to be significantly higher 14 days after $Vasn$ deletion in $Vasn^{SMMHC-CRE-ERT2}$ ^{KO} mice (3.94 ± 1.09 ng/ml, $p < 0.005$ vs. other groups) and trend to lower at 21 days (1.35 ± 0.06 ng/ml, NS). Serum endothelin 1 levels did not change significantly in any of the groups (Supporting Information: Table 3).

We observed no mortality at 21 days for Aged $Vasn^{CRE-ERT}$ ^{KO} mice. The Aged $Vasn^{CRE-ERT}$ ^{KO} mice displayed significantly lower systolic, diastolic, and mean arterial blood pressure and heart rate 21 days after tamoxifen injection (Figure 2d) but none showed a
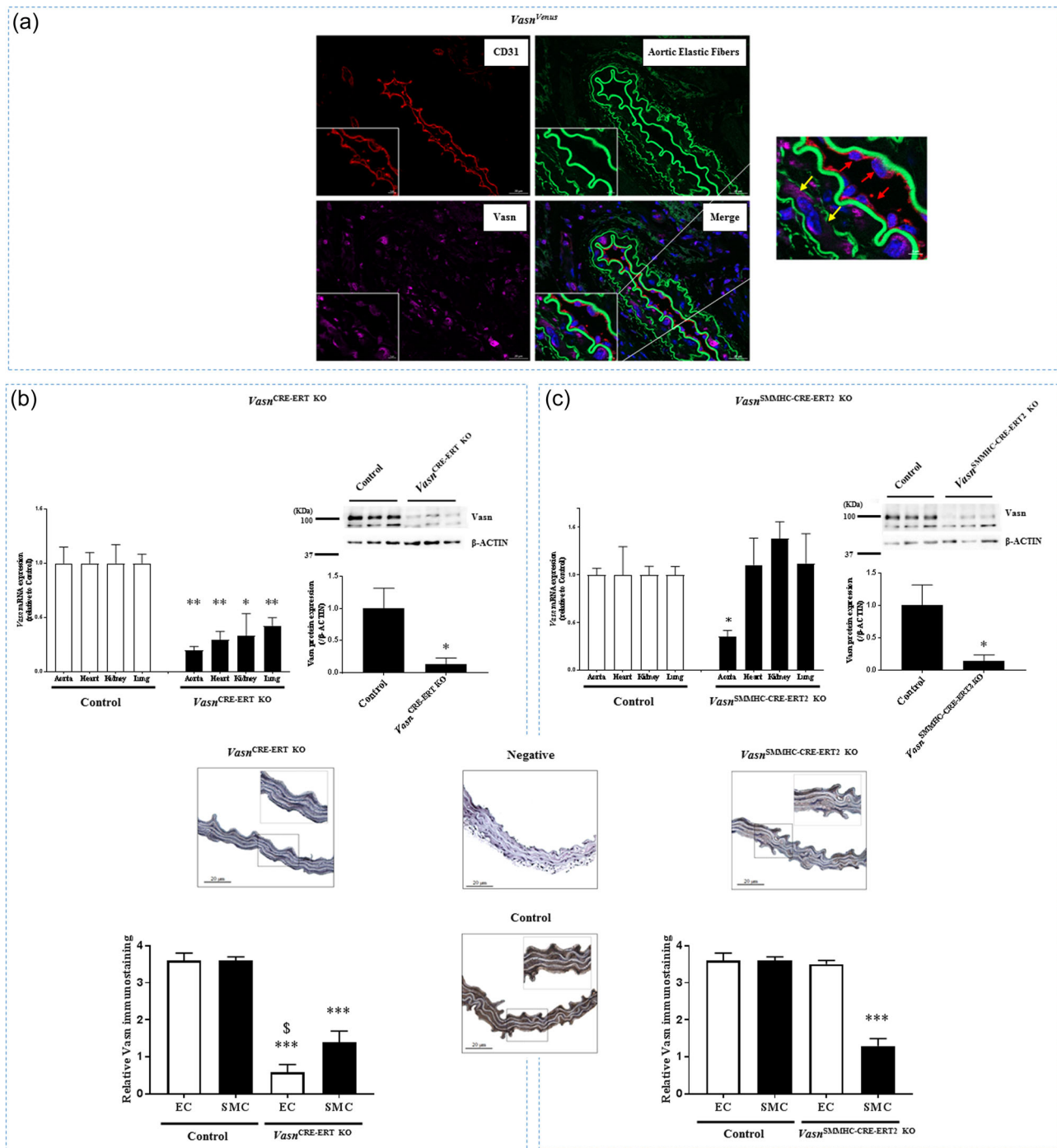
FIGURE 1 Vasn expression in ECs, SMCs, aorta, and organs of $Vasn^{\text{CRE-ERT KO}}$ and $Vasn^{\text{SMMHC-CRE-ERT2 KO}}$ mice. (a) Sections of aorta from a $Vasn^{Venus}$ transgenic mouse. Immunofluorescence of ECs (CD31; red), aortic elastic fibers (green) and Venus$^+$ cells (pink). Nuclei were counterstained with Hoechst reagent (blue). The red arrow indicates Venus-positive ECs, and the yellow arrow indicates Venus-positive SMCs. In $Vasn^{\text{CRE-ERT KO}}$ mice (b) and $Vasn^{\text{SMMHC-CRE-ERT2 KO}}$ mice (c), total RNA from thoracic aortas, heart, kidney, and lung were measured and compared with control mice. Vasn protein expression in aortas was assessed in Western blots and compared with extracts from control mice. Representative immunoblots show the inhibition of Vasn protein synthesis. Quantification of Vasn expression in ECs and SMCs using Vasn immunostaining, scored from 0 (absence of immunostaining) to 4 (greatest possible immunostaining). In all qPCR experiments, Gapdh was used as the internal reference gene. For Vasn immunostaining, five thoracic aorta sections were averaged for each animal. EC, endothelial cell; SMC, smooth muscle cell. Negative control (Negative) corresponds to immunostaining without the primary anti-Vasn antibody. Vasn protein expression was quantified and normalized against β-ACTIN. Control mice $n = 4–6$, $Vasn^{\text{CRE-ERT KO}}$ $n = 5$, $Vasn^{\text{SMMHC-CRE-ERT2 KO}}$ $n = 4$. $*p < 0.05$, $**p < 0.01$, $***p < 0.001$ versus control, $\$p < 0.001$ versus EC of $Vasn^{\text{SMMHC-CRE-ERT2 KO}}$ mice.

FIGURE 2 Effect of *Vasn* deletion on arterial blood pressure, heart rate, and Ang II levels in *Vasn*[CRE-ERT KO] and *Vasn*[SMMHC-CRE-ERT2 KO] mice. Systolic, diastolic, and mean arterial blood pressures and heart rate 21 days after tamoxifen injection in (a) 8-week-old *Vasn*[CRE-ERT KO] (b) 8-week-old *Vasn*[SMMHC-CRE-ERT2 KO] mice and (d) 1-year-old (Aged) *Vasn*[CRE-ERT KO] mice. The results correspond to cumulative data from 13 to 16 control mice, 17 *Vasn*[CRE-ERT KO] mice, 16 *Vasn*[SMMHC-CRE-ERT2 KO] mice, and 4 Aged *Vasn*[CRE-ERT KO] mice. $*p < 0.05$, $**p < 0.01$, $***p < 0.0005$, $****p < 0.0001$ versus controls. (c) Ang II levels in control, *Vasn*[CRE-ERT KO] and *Vasn*[SMMHC-CRE-ERT2 KO] mice after 14 days (D14) and 21 days (D21). Control mice $n = 12$, *Vasn*[CRE-ERT KO] D14 $n = 6$, *Vasn*[CRE-ERT KO] D21 $n = 10$, *Vasn*[SMMHC-CRE-ERT2 KO] D14 $n = 6$, *Vasn*[SMMHC-CRE-ERT2 KO] D21 $n = 10$. $*p < 0.05$, $**p < 0.005$ versus control mice. $\$\$\$\$p < 0.0001$ versus *Vasn*[CRE-ERT KO] D14. $£££p < 0.0005$ versus *Vasn*[SMMHC-CRE-ERT2 KO] D21.

dramatic decrease in these parameters to the point of lethality as that observed for *Vasn*[CRE-ERT KO] mice.

3.4 | Impact of *Van* deletion on vascular function

In *Vasn*[CRE-ERT KO] mice, the significantly lower systolic, diastolic, and mean arterial blood pressure values, heart rate, and Ang II levels at 21 days were concomitant with a decrease in endothelium-dependent relaxation response to acetylcholine ($p < 0.0005$ vs. control mice, this alteration of relaxation was observed from 14 days) and with a decrease in ability of vessel to contract in response to phenylephrine ($p < 0.0005$ vs. control mice, Figure 3a).

In *Vasn*[SMMHC-CRE-ERT2 KO] mice, the elevated Ang II level at 14 days was simultaneous with a significantly stronger contraction response to phenylephrine ($p < 0.05$ vs. control mice, Figure 3b). At 21 days, the nonsignificant decrease in Ang II levels was synchronous

to a reduction of contraction in response to phenylephrine ($p < 0.05$ vs. control mice, Figure 3b).

In line with these findings *Vasn*[SMMHC-CRE-ERT2 KO] mice at 14 and 21 days, the Ang II level was significantly correlated with the response to phenylephrine ($r^2 = 0.56$, $p < 0.05$, Figure 3c). We, therefore, used immunoblotting to measure the aortic expression of the Ang II receptor (AT1) in our models 21 days after induction; there were no significant changes between either *Vasn*[CRE-ERT KO] or *Vasn*[SMMHC-CRE-ERT2 KO] mice *versus* controls (Supporting Information: Figure S1).

In view of the role of myosin phosphatase target subunit 1 (MYPT1) in regulating the contraction of SMCs, we also studied the protein's activity. The impaired contractibility observed in *Vasn*[CRE-ERT KO] and *Vasn*[SMMHC-CRE-ERT2 KO] mice was associated with a low level of p-MYPT1, with 50% and 42% reductions, respectively ($p < 0.05$, Figure 3d).

Moreover, a significantly weaker endothelium-dependent relaxation response to acetylcholine was observed in *Vasn*[SMMHC-CRE-ERT2 KO] mice
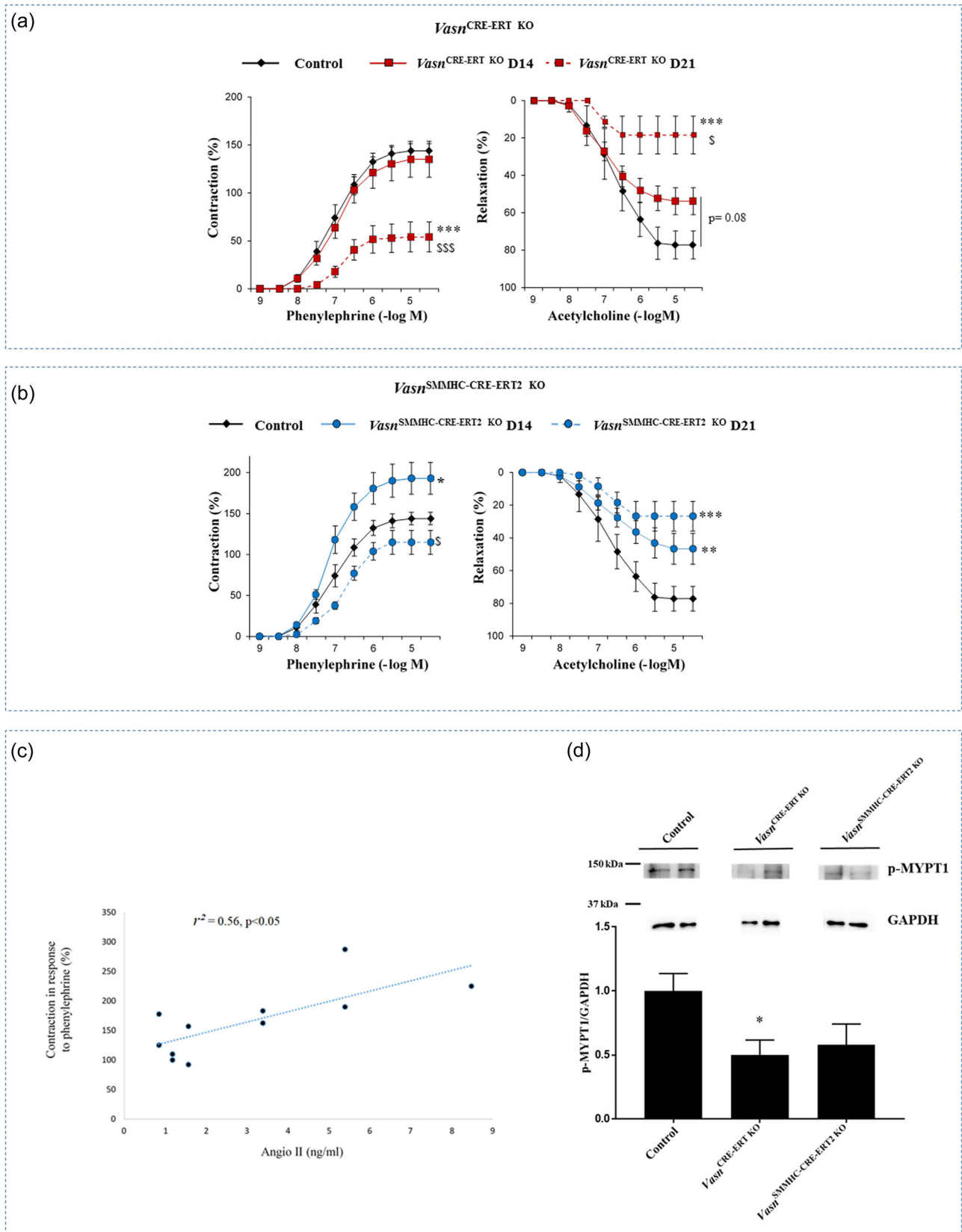
FIGURE 3 (See caption on next page)

at 14 days ($p < 0.005$ vs. control mice) and even more so at 21 days ($p < 0.0005$ vs. control mice, Figure 3b).

3.5 | *VASN* silencing modulates the HVSMC phenotype

To investigate the weaker contractile responses to phenylephrine, we studied a model of *VASN* silencing in HVSMCs. Treatment with siVasn was associated with significantly lower levels of *VASN* mRNA (-50%, $p < 0.0001$) and VASN protein (-42.5%, $p < 0.05$) versus siNeg (Figure 4a). The cell viability was found to not significantly trend to lower after *VASN* silencing.

In this HVSMC model, *VASN* silencing induced a switch toward the contractile phenotype; this was evidenced by a significant relative reduction in the expression of genes associated with the synthetic phenotype: collagen 8 (Coll8, -3.6%, $p < 0.05$), collagen 1 (Coll1, -21.5%, $p < 0.0001$), and osteopontin (OPN, -30%, $p < 0.05$; Figure 4b) and a significant relative increase in the expression of genes associated with a contractile phenotype: calponin-1 (CNN1, $+20\%$, $p < 0.01$), α-smooth muscle actin (α-SMA, $+37\%$, $p < 0.0001$) and smooth muscle myosin heavy chains (SMMHC, $+76\%$, $p < 0.0001$; Figure 4c).

Our experiments evidenced significantly lower levels of pSTAT3 (vs. controls) in vessels from *Vasn*[CRE-ERT KO] mice and *Vasn*[SMMHC-CRE-ERT2 KO] mice (-68%, $p < 0.01$; and -72%, $p < 0.05$, Figure 4d).

3.6 | *VASN* silencing decreases the HVSMCs ability to respond to contraction inductor: Actions on basal calcium entry and basal calcium concentration

We next measured the effect of carbachol (a muscarinic agonist that induces Ca^{2+} release and thus SMC contraction) on siVasn-transfected HVSMCs. The latter cells were less able than control cells to generate a calcium signal in response to carbachol: the response frequency was 44.7% lower ($p < 0.001$) in the siVasn condition than in the siNeg condition (Figure 5a). To complement the above-mentioned vascular responsiveness experiments, we assayed the HVSMCs' metabotropic Ca^{2+} response to the adrenergic agonist phenylephrine. As had been seen for carbachol stimulation, fewer siVasn-transfected HVSMCs responded to phenylephrine stimulation, and the level of response was lower than controls. This lack of responsiveness was not due to the regulation of metabotropic receptors: mRNA levels of the HVSMC-predominant muscarinic receptors (CHRM2 and CHRM3) and adrenergic receptors (ADRA1A, ADRA1B, and ADRA1D) were not found to be significantly up- or downregulated (Supporting Information: Figure S2).

After calibration with a calcium standard, we found that the intracellular Ca^{2+} response was significantly weaker in the siVasn condition (75.8 nM) than in the siNeg condition (1564.5 nM; $p < 0.001$). This effect was associated with a significant relative increase (by 54.7%) in the basal Ca^{2+} concentration in the siVasn condition (275.6 ± 20.2 nM), compared with siNeg control cells (178.1 ± 10.2 nM; $p < 0.001$, Figure 5b).

The quenching of fura-2 fluorescence by Mn^{2+} was used to study Ca^{2+} entry into the cell. Mn^{2+} enters the cell via plasma membrane Ca^{2+} channels and accumulates in the cytosol because it is poorly accepted by other cellular transport systems. A decrease over time in fura-2 fluorescence reveals Mn^{2+} influx through plasma membrane Ca^{2+} channels. In our experiments, the quench slope was significantly steeper in siVasn HVSMCs than in siNeg control cells, meaning that fluorescence was decreasing faster; hence, membrane permeability to divalent cations was higher in siVasn-transfected cells (Figure 5c).

To study basal Ca^{2+} entry further, HVSMCs were exposed to a Ca^{2+}-free solution (to reduce $[Ca^{2+}]_i$) and then a Ca^{2+}-containing solution (to test Ca^{2+} entry). Basal Ca^{2+} entry was significantly higher in siVasn-transfected HVSMCs (Figure 5d).

3.7 | Impact of *Vasn* deletion on relaxation signaling pathways

In experiments on the signaling pathways involved in relaxation, we demonstrated that the observed impairment of endothelial relaxation was associated with lower levels of AKT and eNOS activation in both inducible KO models as assessed by p-AKT/AKT and p-eNOS/eNOS ratio (45% relative reduction in both models, $p < 0.05$; Figure 6a,b). The ADMA levels were similar in all groups of mice (Figure 6c). Although we validated the decrease of VASN expression in *VASN*-silenced HUVECs (-45%, $p < 0.05$ for mRNA; -52%, $p < 0.05$ for

---

FIGURE 3 Impact of *Vasn* deletion on vascular function in *Vasn*[CRE-ERT KO] and *Vasn*[SMMHC-CRE-ERT2 KO] mice, and correlation between Ang II levels and contraction in *Vasn*[SMMHC-CRE-ERT2 KO] mice. (a) Contraction obtained with phenylephrine and relaxation obtained with acetylcholine in *Vasn*[CRE-ERT KO] mouse vessels 14 days (*Vasn*[CRE-ERT KO] D14, $n = 8$) and 21 days (*Vasn*[CRE-ERT KO] D21, $n = 8$) after *Vasn* KO. (b) Contraction obtained with phenylephrine and relaxation obtained with acetylcholine in *Vasn*[SMMHC-CRE-ERT2 KO] mouse vessels 14 days (*Vasn*[SMMHC-CRE-ERT2 KO] D14, $n = 7$) and 21 days (*Vasn*[SMMHC-CRE-ERT2 KO] D21, $n = 4$) after *Vasn* KO. Control mice $n = 7$. *$p < 0.05$, **$p < 0.005$, ***$p < 0.0005$ versus control mice; $$p < 0.01$, $$$$p < 0.0001$ versus D14 group. (c) Correlation between the contraction in response to phenylephrine and Ang II levels in *Vasn*[SMMHC-CRE-ERT2 KO] mice at 14 days and 21 days. Control mice $n = 12$, *Vasn*[SMMHC-CRE-ERT2 KO] D14 $n = 6$, *Vasn*[SMMHC-CRE-ERT2 KO] D21 $n = 10$. (d) p-MYPT1 protein expression levels in aortas from *Vasn*[CRE-ERT KO] and *Vasn*[SMMHC-CRE-ERT2 KO] mice were assessed using Western blot analysis and compared with extracts from control mice ($n = 6$, for each condition). *$p < 0.05$, versus control mice.

(a)
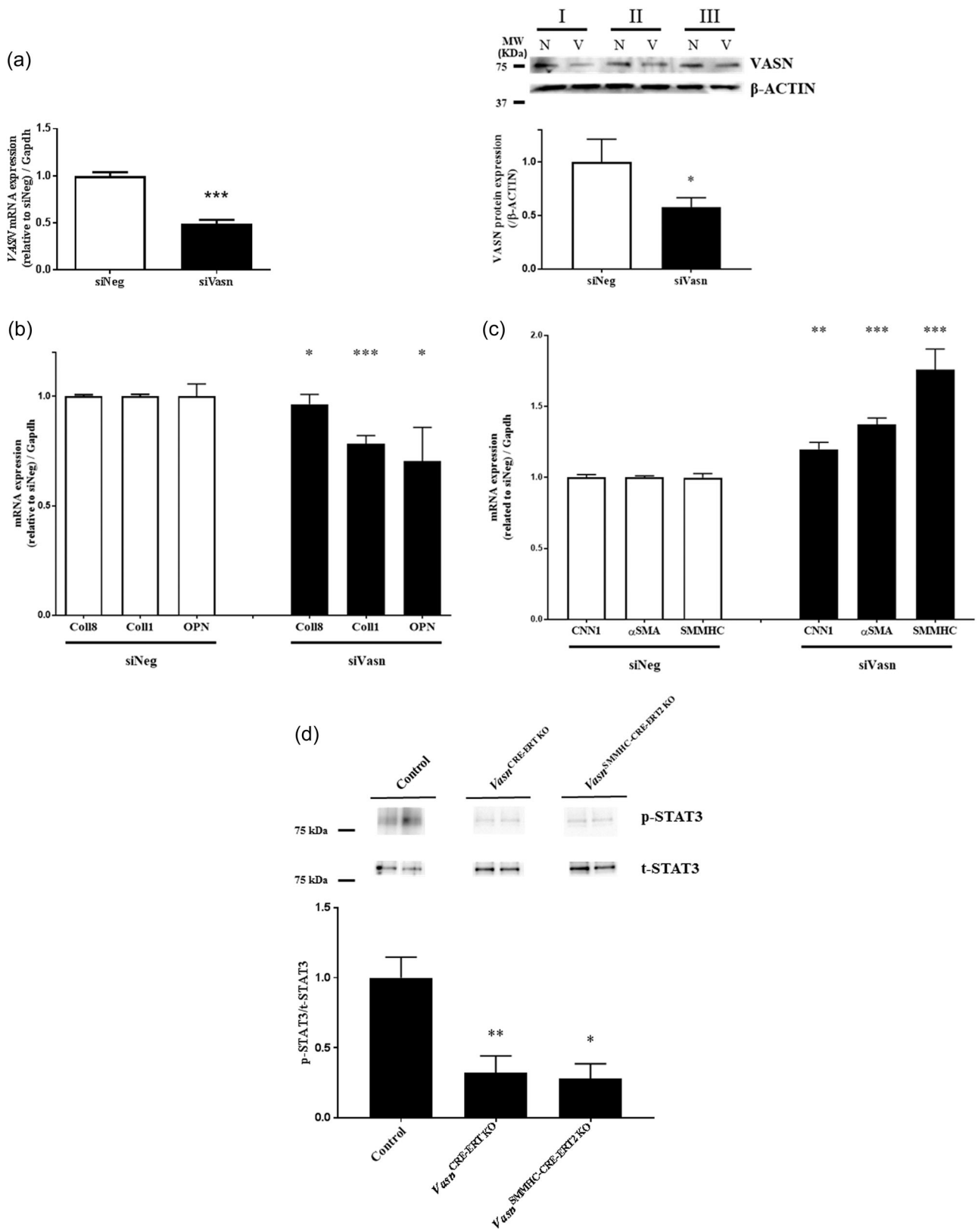

(b)

(c)

(d)

FIGURE 4   (See caption on next page)

protein), we noticed that VASN vanished during successive passages of HUVECs and that efficient inhibition of VASN expression could only be obtained for passages 2–4. The decrease of *VASN* expression (−57%, $p < 0.05$) and VASN protein levels (−46%, $p < 0.05$) reached statistical significance at passage 6 (Figure 6d), whereas the viability of *VASN*-silenced HUVECs remained unchanged. The relaxation signaling pathway was highly and significantly affected in HUVECs, with eNOS activation significantly inhibited (−31%, $p < 0.05$; Figure 6e), similar to what was found for aortas. To complete these results, we measured NO production in HUVECs with DAF-FM DA and observed significantly lower NO production by *VASN*-silenced HUVECs than by siNeg and control cells (−21%, $p < 0.05$).

4 | DISCUSSION

The fact that the $Vasn^{-/-}$ mice died around 21 days of life and the $Vasn^{CRE-ERT\ KO}$ mice died 21 days after the induction of *Vasn* deletion demonstrates that vasorin has a major physiological role. Our present findings explain the dramatic effect of *Vasn* deletion on vascular function. In mice, *Vasn* KO was associated with impairment in contraction and endothelium-dependent relaxation. The results of our mechanistic experiments suggest that vasorin has two major functional roles in SMCs and ECs. In fact, the vascular dysfunction caused by *Vasn* deletion is mediated by Ang II levels, SMC phenotype switching, and changes in intracellular calcium homeostasis and ECs
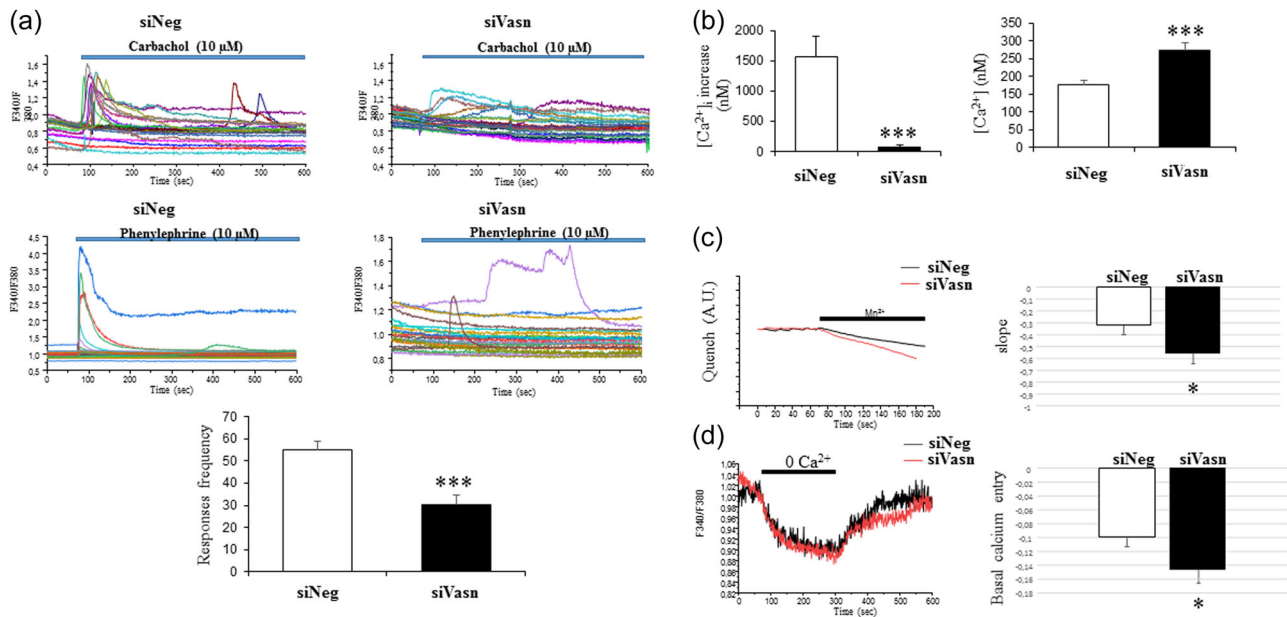
FIGURE 5 Effect of *VASN* silencing on calcium homeostasis in HVSMCs. (a) Typical frequency responses obtained to carbachol or phenylephrine stimulation in silenced (siVasn-transfected cells) and control (scrambled siRNA, siNeg) cells ($n = 45$ cells). (b) Magnitude of Ca^{2+} responses and the basal Ca^{2+} concentration in siVasn-transfected cells ($n = 245$) and siNeg control cells ($n = 250$). (c) Recordings of the extracellular application of Mn^{2+} (quenching the Fura-2 fluorescent probe) and analysis of the corresponding slopes (siNeg, $n = 32$; siVasn, $n = 24$) in transfected HVSMCs. (d) Typical recordings of basal entry of Ca^{2+} and quantification in siNeg-transfected HVSMCs ($n = 19$) and siVasn transfected HVSMCs ($n = 21$). HVSMC, human vascular smooth muscle cell. *$p < 0.05$, ***$p < 0.001$ versus siNeg.

FIGURE 4 Influence of *Vasn* silencing on SMC phenotypic marker expression and STAT3 activation in aortic samples from $Vasn^{CRE-ERT\ KO}$ and $Vasn^{SMMHC-CRE-ERT2\ KO}$ mice. (a) mRNA expression in silenced (siVasn-transfected) HVSMCs versus control cells treated with a scrambled siRNA (siNeg), representative Western blots of VASN protein expression, and quantification of VASN protein expression in siRNA-transfected HVSMCs from six donors ($n = 6$); I, II and III are different donors; N and V correspond to the siNeg and siVasn conditions, respectively. (b) mRNA expression of collagen 8 (Coll8), collagen 1 (Coll1), and osteopontin (OPN) was analyzed using qPCR in siVasn HVSMCs and compared with control cells (siNeg). (c) mRNA expression of calponin (CNN1), α-smooth muscle actin (α-SMA), and smooth muscle myosin heavy chains (SMMHCs) was analyzed using qPCR in siVasn HVSMCs and compared with control cells (siNeg). For all mRNA expression analyses, the results correspond to cumulative data from two independent reverse transcriptions of total RNA from six donors ($n = 12$). The value in the siNeg condition was set to 1. *$p < 0.05$, **$p < 0.01$, ***$p < 0.0001$ versus siNeg. (d) STAT3 protein expression and activation in aorta samples from $Vasn^{CRE-ERT\ KO}$ and $Vasn^{SMMHC-CRE-ERT2\ KO}$ mice was assessed in Western blots and compared with extracts of aortas from control mice ($n = 6$, for each condition). The expression of the phosphorylated form of STAT3 (p-STAT3) was quantified and normalized against total STAT3 (t-STAT3). Representative immunoblots are shown above the quantification histograms. HVSMC, human vascular smooth muscle cell. *$p < 0.05$, **$p < 0.01$ versus control mice.
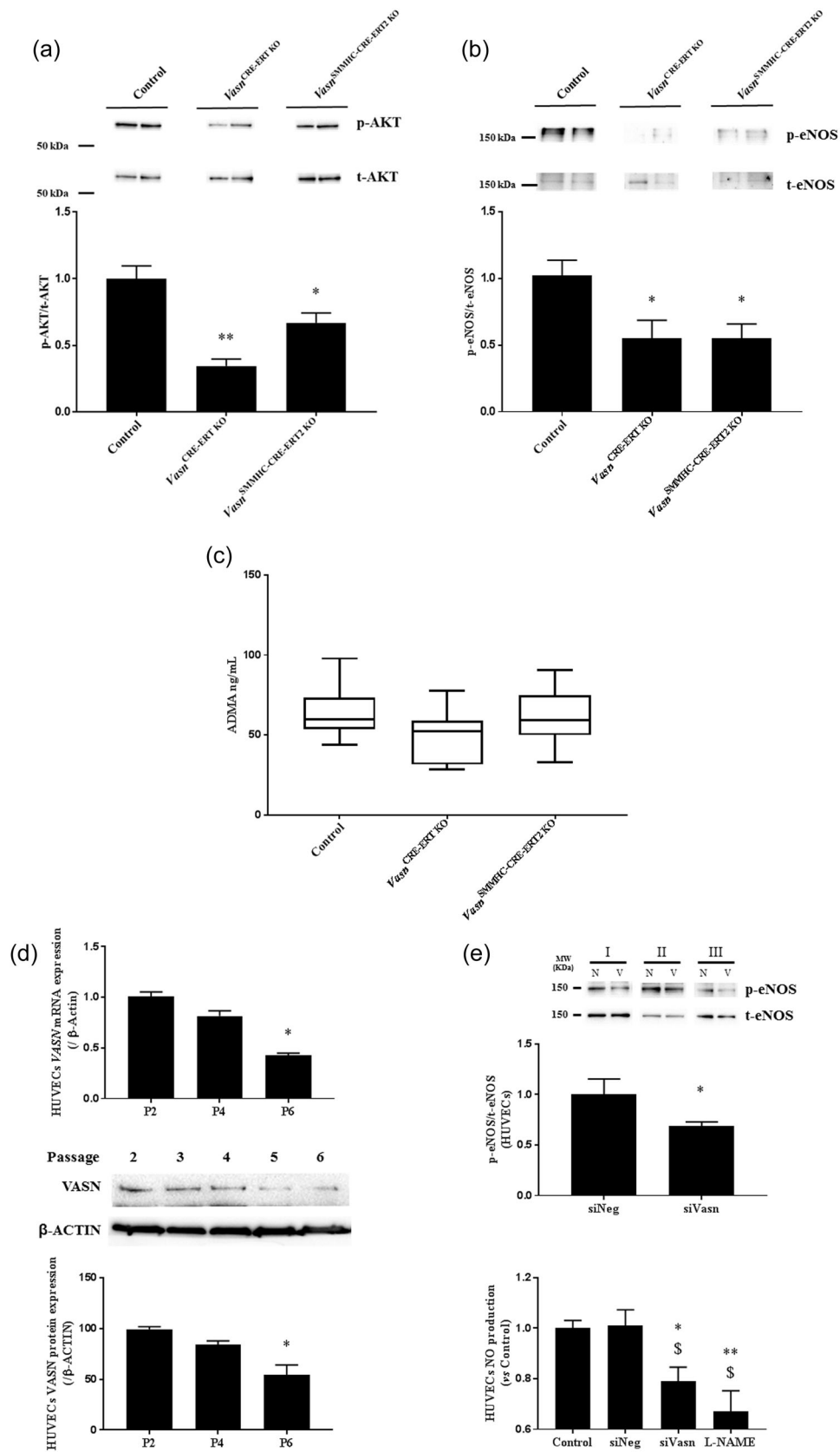
FIGURE 6 (See caption on next page)

NO signaling. A recent study suggested that cardiac hypertrophy was the cause of death in $Vasn^{-/-}$ mice (Sun et al., 2022). Our results indicated that the harmful impact of $Vasn$ deletion on vascular function might also contribute to the high observed mortality rate.

The death of $Vasn^{CRE-ERT\ KO}$ mice 21 days after tamoxifen injection and $Vasn$ KO induction was preceded by low heart rate and blood pressure values, low levels of Ang II (the octapeptide produced by cleavage of Ang I by angiotensin-converting enzyme 1), and poor vascular contractibility. Ang II is a powerful vasoconstrictor and is involved in the regulation of blood pressure (by binding to the AT1 receptor), the induction of vasoconstriction, the release of anti-diuretic and adrenocorticotropin hormones, and direct effects on the sympathetic system (Campbell, 2013). Pintus et al. (2018) reported that the arterial wall's vasorin content fell with age, and that this change was associated with greater Ang II signaling. Our study involved young animals; in this context, low Vasn expression in SMCs was associated with elevated Ang II levels at 14 days. Furthermore, low Vasn expression in all tissues was associated with low Ang II levels. Vasn is strongly expressed by SMCs but it was also expressed by ECs and in the liver and the kidneys—organs in which Vasn's role in the regulation of the renin–angiotensin system has yet to be studied. Our results also showed that the role of Vasn expression depends on age. The deletion of $Vasn$ in young mice led to changes in blood pressure and induce mortality at 21 days, whereas $Vasn$ deletion in aged mice had no effect on mortality.

A deficit in contraction of the vessel can lead to severe low blood pressure, known as vasoplegic shock. Shock occurs when blood vessels relax to the point where they are no longer able to properly maintain blood flow. Indeed, it has been demonstrated that low levels of Ang II are associated with elevated mortality in cases of severe sepsis (Zhang, 2014) and vasodilatory shock (Rice et al., 1983). In the United States and Europe, synthetic human Ang II has been approved for increasing blood pressure in patients with vasodilatory shock (Senatore et al., 2019). In the present study, low levels of Ang II were associated with the poor contractibility of isolated aorta, to an extent that would prevent the proper maintenance of blood flow. Low Ang II levels are harmful when abnormal vasodilatation has to be counterbalanced.

The observed defect of contraction in response to phenylephrine can also reflect the abnormally high production of vasodilator factors (Lee et al., 2020). In the present study, we observed impaired relaxation in response to acetylcholine and poor eNOS activation; hence, the NO pathway was not associated with the lack of contraction, and other relaxant pathways must be considered.

Impairments in arterial contraction may also be related to the number of VSMCs in the arterial wall. In our study, cell viability was not significantly lower after $VASN$ silencing but our preliminary data revealed a trend for a reduction in media area of $Vasn^{CRE-ERT\ KO}$ mice aortas. Other mechanisms (such as SMC phenotype switching and the release of $[Ca^{2+}]$ in SMCs) are involved in vascular contraction. In our study, the VSMC phenotype switch induced by $VASN$ deletion was concomitant with changes in STAT3 activation. The inhibition of STAT3 activation was associated with the upregulated expression of genes related to the contractile phenotype (Liao et al., 2015).

Moreover, $VASN$ silencing was associated with an elevated basal $[Ca^{2+}]_i$ (276 nM, vs. 178 nM in control cells) and weaker metabotropic responses to carbachol and phenylephrine. There are two possible explanations for the HVSMCs' lack of excitability and poor responsiveness. First, efficient relaxation requires a return to the basal $[Ca^{2+}]_i$; silenced $VASN$ HVSMCs might not fully relax after contraction and so might not be able to respond optimally to subsequent contraction signals. Second, the observed alterations in calcium homeostasis might also lead to desensitization of metabotropic receptors and impact the activity of plasma membrane calcium channels (voltage-operated channels, receptor-operated channels, and transient receptor potential channels), Na^+/Ca^{2+} exchangers, and Ca^{2+}-ATPases or might regulate gene transcription in smooth muscle, as reported in the literature (Bravo-Sagua et al., 2020). These hypotheses require further investigation.

It is noteworthy that the stronger contraction response to phenylephrine at 14 days in $Vasn^{SMMHC-CRE-ERT2\ KO}$ mice was concomitant with an increase in Ang II levels. Vasoactive peptides like Ang II lead to the activation of phospholipase C and thus to inositol trisphosphate production and smooth muscle contraction. The selective α1-adrenergic agonist phenylephrine uses the same

FIGURE 6 Western blot analysis of relaxation signaling pathways in aortas (a–c) of $Vasn^{CRE-ERT\ KO}$ and $Vasn^{SMMHC-CRE-ERT2\ KO}$ mice, and (d,e) HUVECs. Protein expression in aortas from $Vasn^{CRE-ERT\ KO}$ and $Vasn^{SMMHC-CRE-ERT2\ KO}$ mice was assessed using Western blots of selected markers and compared with extracts from control mice ($n = 6$ for each condition). The expression of the phosphorylated forms of AKT and eNOS proteins (p-AKT and p-eNOS) was quantified and normalized against the total protein forms (t-AKT and t-eNOS). Representative immunoblots are shown above each quantification histogram. (a) p-AKT expression in $Vasn^{CRE-ERT\ KO}$ and $Vasn^{SMMHC-CRE-ERT2\ KO}$ mice. (b) p-eNOS expression in $Vasn^{CRE-ERT\ KO}$ and $Vasn^{SMMHC-CRE-ERT2\ KO}$ KO mice. $*p < 0.05$, $**p < 0.01$ versus control mice. (c) ADMA levels in the different mice groups ($n = 15$–16). (d) $VASN$ mRNA expression and VASN protein expression in HUVECs through passages (P). Results represent the accumulated data of independent qPCR experiments ($n = 5$) and the accumulated data of independent Western blot experiments ($n = 3$). The P2 condition was set to 1, $*p < 0.05$ versus P2. (e) The expression of the phosphorylated and total forms of eNOS proteins (p-eNOS and t-eNOS) was assessed by Western blot analysis. Activated p-eNOS levels were quantified and normalized against those of t-eNOS. I, II, and III indicate different independent HUVECs experiments; N and V correspond to the siNeg and siVasn conditions, respectively. Results represent the accumulated data of independent experiments ($n = 4$). The siNeg condition was set to 1, $*p < 0.05$ versus siNeg. NO production in $VASN$-silenced HUVECs. NO production was assessed by measuring the fluorescence of DAF-FM DA. Results represent the accumulated data of HUVECs independent experiments ($n = 7$). The Control condition was set to 1. HUVEC, human umbilical vein endothelial cell. $*p < 0.05$, $**p < 0.01$ versus Control, $p < 0.05$ versus siNeg.

pathway as Ang II to induce smooth muscle cell contraction. The stronger contraction obtained in response to phenylephrine might reflect induction of the SMC contractile state induced by high Ang II levels.

Vascular dysfunction can be caused by an imbalance between levels of vasodilators and levels of vasoconstrictors. In our models, *Vasn* deletion was associated with poor vascular relaxation in response to acetylcholine. The NO pathway is one of the most important pathways in vessel relaxation. In our two *Vasn* KO models, we observed poor eNOS activation and low AKT phosphorylation in the aorta. These results were confirmed in *VASN*-silenced HUVECs, in which the inhibition of *VASN* expression was associated with poor eNOS activation. Furthermore, we demonstrated that the level of NO production was significantly lower and impaired the relaxation pathway. The protein kinase AKT notably contributes to vascular relaxation by mediating NO production via the direct phosphorylation of eNOS (Fulton et al., 1999). Moreover, AKT signaling is essential for many of the ECs' responses, such as the survival-promoting matrix attachment-mediated signaling pathway (Fujio & Walsh, 1999) and vascular permeability (Six et al., 2002). A low NO level is one of the earliest manifestations of endothelial dysfunction. It is noteworthy that the decreases in relaxation were not associated with elevated levels of the endogenous competitive inhibitor of NOS, ADMA. Understanding the NO deficiency observed in *Vasn* KO mice will require further studies.

There is evidence to suggest that *Vasn* expression in the murine arterial wall and in VSMCs falls significantly with age (Pintus et al., 2018). In the arterial walls of aged animals, low Vasn expression is associated with an increase in Ang II signaling. During aging, low Vasn levels promote inflammation (including fibrosis and the activation of MMP-2), whereas elevated Vasn expression is anti-inflammatory and anti-fibrotic (Pintus et al., 2018). Like elevated Ang II production and low NO levels, low Vasn expression in the aging arterial wall is starting to be seen as a pro-inflammatory, profibrotic factor that leads to fibrosis (Wang et al., 2020). Vasorin appears to have a different role in the arterial walls of young animals. We observed that the deletion of Vasn leads to death after 21 days in young mice but does not in aged mice. Furthermore, the repercussions of Vasn deletion on blood pressure and vascular dysfunction were less dramatic in older mice than in young mice. Our data and those reported by Pintus et al. strongly suggest that vasorin has several roles and that its expression appears to be essential (essentially for vascular function) in young animals. Further research is likely to reveal additional details of the vasorin's fundamental role in cardiovascular disease. At the cellular level, the course of vasorin expression was strikingly different in cultures of HVSMCs versus cultures of HUVECs. *Vasn* expression remained stable from passage 3 to 12 in HVSMCs, whereas it had fallen significantly by passage 6 in HUVECs—suggesting that ECs have a distinct role in the vasorin-related effects observed in aging vessels.

It is noteworthy that the *Vasn*[CRE-ERT KO] mice displayed excessive body weight gain 21 days after tamoxifen injection. This appeared to be due to edema because the latter were not observed in the other groups of mice. The animal's cardiac function warrants investigation, to determine whether cardiac insufficiency is responsible for the observed edema. Alternatively, the edemas might have been linked to renal insufficiency; the high level of vasorin expression in the kidney suggests that *Vasn* KO would have an impact on this organ. These questions will also have to be addressed in future research.

The present study had a number of limitations and strengths. The main limitation was the use of the tail-cuff method (rather than telemetry) to measure blood pressure. The strengths include (i) the use of *Vasn*[CRE-ERT KO] and *Vasn*[SMMHC-CRE-ERT2 KO] mice (enabling us to analyze the consequences of respectively total or SMC-selective *Vasn* KO on vascular function), (ii) our analysis of a number of variables 14 days and 21 days after *Vasn* deletion, (iii) the measurement of vascular reactivity ex vivo, and (iv) the *VASN* silencing in human VSMCs and ECs.

In conclusion, our present results revealed vasorin's fundamental role in vascular function and blood pressure homeostasis via modulation of eNOS activation, the VSMC phenotype, intracellular calcium levels, and Ang II levels. Our results prompted us to hypothesize that the absence of vasorin in the blood vessel leads to low NO production and endothelial dysfunction (due to effects on ECs) and impairments of contraction and relaxation (also due to effects on VSMCs). Vasorin might therefore be a novel therapeutic target in vascular dysfunction and cardiovascular disease.

AUTHOR CONTRIBUTIONS

Isabelle Six, Loïc Louvet, and Gaëlle Lenglet conceived the hypotheses and analyses. Heinrich Schrewe, A. Michaela Krautzberger, and Catherine Chaussain provided mice and antibodies and helped to conceive the experimental techniques. Romuald Mentaverri helped to develop transgenic models. Isabelle Six, Loïc Louvet, Gaëlle Lenglet, Frédéric Hague, Clara Kowalewski, Julie Lesieur, and Nassim Mahtal collected samples and data. Isabelle Six, Loïc Louvet, Gaëlle Lenglet, Frédéric Hague, Clara Kowalewski, Cathy Gomila, and Nassim Mahtal conducted the experiments. Isabelle Six, Loïc Louvet, and Gaëlle Lenglet performed statistical analysis and drafted the paper. Romuald Mentaverri, Anne-Laure Bonnet, Caroline Andrique, Céline Gaucher, Nassim Mahtal, Pierre-Louis Tharaux, Said Kamel, and Catherine Chaussain refined the interpretation and the final manuscript. All the authors have accepted responsibility for the entire content of this submitted manuscript and approved submission.

ACKNOWLEDGMENTS

CONFLICT OF INTEREST

The authors declare no conflicts of interest.

ORCID

Romuald Mentaverri http://orcid.org/0000-0002-3993-1561

Isabelle Six http://orcid.org/0000-0002-5256-8138

REFERENCES

Bonnet, A. L., Chaussain, C., Broutin, I., Rochefort, G. Y., Schrewe, H., & Gaucher, C. (2018). From vascular smooth muscle cells to folliculogenesis: What about vasorin? *Frontiers of Medicine*, 5, 335. https://doi.org/10.3389/fmed.2018.00335

Bravo-Sagua, R., Parra, V., Muñoz-Cordova, F., Sanchez-Aguilera, P., Garrido, V., Contreras-Ferrat, A., Chiong, M., & Lavandero, S. (2020). Sarcoplasmic reticulum and calcium signaling in muscle cells: Homeostasis and disease. *International Review of Cell and Molecular Biology*, 350, 197–264. https://doi.org/10.1016/bs.ircmb.2019.12.007

Campbell, D. J. (2013). Do intravenous and subcutaneous angiotensin II increase blood pressure by different mechanisms? *Clinical and Experimental Pharmacology and Physiology*, 40(8), 560–570. https://doi.org/10.1111/1440-1681.12085

Choksi, S., Lin, Y., Pobezinskaya, Y., Chen, L., Park, C., Morgan, M., Li, T., Jitkaew, S., Cao, X., Kim, Y. S., Kim, H. S., Levitt, P., Shih, G., Birre, M., Deng, C. X., & Liu, Z. G. (2011). A HIF-1 target, ATIA, protects cells from apoptosis by modulating the mitochondrial thioredoxin, TRX2. *Molecular Cell*, 42(5), 597–609. https://doi.org/10.1016/j.molcel.2011.03.030

Daya, H. A., Kouba, S., Ouled-Haddou, H., Benzerdjeb, N., Telliez, M. S., Dayen, C., Sevestre, H., Garçon, L., Hague, F., & Ouadid-Ahidouch, H. (2021). Orai3-mediates cisplatin-resistance in non-small cell lung cancer cells by enriching cancer stem cell population through PI3K/AKT pathway. *Cancers*, 13(10), 2314. https://doi.org/10.3390/cancers13102314

Fujio, Y., & Walsh, K. (1999). Akt mediates cytoprotection of endothelial cells by vascular endothelial growth factor in an anchorage-dependent manner. *Journal of Biological Chemistry*, 274(23), 16349–16354. https://doi.org/10.1074/jbc.274.23.16349

Fulton, D., Gratton, J. P., McCabe, T. J., Fontana, J., Fujio, Y., Walsh, K., Franke, T. F., Papapetropoulos, A., & Sessa, W. C. (1999). Regulation of endothelium-derived nitric oxide production by the protein kinase Akt. *Nature*, 399(6736), 597–60. https://doi.org/10.1038/21218

Huang, A., Dong, J., Li, S., Wang, C., Ding, H., Li, H., Su, X., Ge, X., Sun, L., Bai, C., Shen, X., Fang, T., Li, J., & Shao, N. (2015). Exosomal transfer of vasorin expressed in hepatocellular carcinoma cells promotes migration of human umbilical vein endothelial cells. *International Journal of Biological Sciences*, 11, 961–969. https://doi.org/10.7150/ijbs.11943

Ikeda, Y., Imai, Y., Kumagai, H., Nosaka, T., Morikawa, Y., Hisaoka, T., Manabe, I., Maemura, K., Nakaoka, T., Imamura, T., Miyazono, K., Komuro, I., Nagai, R., & Kitamura, T. (2004). Vasorin, a transforming growth factor beta-binding protein expressed in vascular smooth muscle cells, modulates the arterial response to injury in vivo. *Proceedings of the National Academy of Sciences of the United States of America*, 101(29), 10732–10737. https://doi.org/10.1073/pnas.0404117101

Krautzberger, A. M., Kosiol, B., Scholze, M., & Schrewe, H. (2012). Expression of vasorin (Vasn) during embryonic development of the mouse. *Gene Expression Patterns*, 12(5–6), 167–171. https://doi.org/10.1016/j.gep.2012.02.003

Lee, S. H., Ok, S. H., Subbarao, R. B., Kim, J. Y., Bae, S. I., Hwang, Y., Tak, S., & Sohn, J. T. (2020). Nitric oxide-mediated inhibition of phenylephrine-induced contraction in response to hypothermia is partially modulated by endothelial Rho-kinase. *International Journal of Medical Sciences*, 17(1), 21–32. https://doi.org/10.7150/ijms.39074

Li, D., Zhang, T., Yang, X., Geng, J., Li, S., Ding, H., Li, H., Huang, A., Wang, C., Sun, L., Bai, C., Zhang, H., Li, J., Dong, J., & Shao, N. (2018). Identification of functional mimotopes of human vasorin ectodomain by biopanning. *International Journal of Biological Sciences*, 14(4), 461–470. https://doi.org/10.7150/ijbs.22692

Liao, X. H., Wang, N., Zhao, D. W., Zheng, D. L., Zheng, L., Xing, W. J., Ma, W. J., Bao, L. Y., Dong, J., & Zhang, T. C. (2015). STAT3 protein regulates vascular smooth muscle cell phenotypic switch by interaction with myocardin. *Journal of Biological Chemistry*, 290(32), 19641–19652. https://doi.org/10.1074/jbc.M114.630111

Louvet, L., Büchel, J., Steppan, S., Passlick-Deetjen, J., & Massy, Z. A. (2013). Magnesium prevents phosphate-induced calcification in human aortic vascular smooth muscle cells. *Nephrology, Dialysis, Transplantation*, 28(4), 869–878. https://doi.org/10.1155/2016/7419524

Maizel, J., Six, I., Slama, M., Tribouilloy, C., Sevestre, H., Poirot, S., Giummelly, P., Atkinson, J., Choukroun, G., Andrejak, M., Kamel, S., Mazière, J. C., & Massy, Z. A. (2009). Mechanisms of aortic and cardiac dysfunction in uremic mice with aortic calcification. *Circulation*, 119(2), 306–313. https://doi.org/10.1161/CIRCULATIONAHA.108.797407

Malapeira, J., Esselens, C., Bech-Serra, J. J., Canals, F., & Arribas, J. (2011). ADAM17 (TACE) regulates TGFβ signaling through the cleavage of vasorin. *Oncogene*, 30(16), 1912–1922. https://doi.org/10.1038/onc.2010.565

Man, J., Yu, X., Huang, H., Zhou, W., Xiang, C., Huang, H., Miele, L., Liu, Z., Bebek, G., Bao, S., & Yu, J. S. (2018). Hypoxic induction of vasorin regulates Notch1 turnover to maintain glioma stem-like cells. *Cell Stem Cell*, 22(1), 104–118.e6. https://doi.org/10.1016/j.stem.2017.10.005

Pintus, G., Giordo, R., Wang, Y., Zhu, W., Kim, S. H., Zhang, L., Ni, L., Zhang, J., Telljohann, R., McGraw, K. R., Monticone, R. E., Ferris, C., Liu, L., Wang, M., & Lakatta, E. G. (2018). Reduced vasorin enhances angiotensin II signaling within the aging arterial wall. *Oncotarget*, 9(43), 27117–27132. https://doi.org/10.18632/oncotarget.25499

Rice, C. L., Kohler, J. P., Casey, L., Szidon, J. P., Daise, M., & Moss, G. S. (1983). Angiotensin-converting enzyme (ACE) in sepsis. *Circulatory Shock*, 11(1), 59–63.

Senatore, F., Jagadeesh, G., Rose, M., Pillai, V. C., Hariharan, S., Liu, Q., McDowell, T. Y., Sapru, M. K., Southworth, M. R., & Stockbridge, N. (2019). FDA approval of angiotensin II for the treatment of hypotension in adults with distributive shock. approbation par la FDA de l'angiotensine II pour le traitement de l'hypotension chez les adultes sous choc distributif. *American Journal of Cardiovascular Drugs: Drugs, Devices, and Other Interventions*, 19(1), 11–20. https://doi.org/10.1007/s40256-018-0297-9

Six, I., Kureishi, Y., Luo, Z., & Walsh, K. (2002). Akt signaling mediates VEGF/VPF vascular permeability in vivo. *FEBS Letters*, 532(1–2), 67–69. https://doi.org/10.1016/s0014-5793(02)03630-x

Six, I., Okazaki, H., Gross, P., Cagnard, J., Boudot, C., Maizel, J., Drueke, T. B., & Massy, Z. A. (2014). Direct, acute effects of Klotho and FGF23 on vascular smooth muscle and endothelium. *PLoS ONE*, 9(4), e93423. https://doi.org/10.1371/journal.pone.0093423

Sun, J., Guo, X., Yu, P., Liang, J., Mo, Z., Zhang, M., Yang, L., Huang, X., Hu, B., Liu, J., Ouyang, Y., & He, M. (2022). Vasorin deficiency leads to cardiac hypertrophy by targeting MYL7 in young mice. *Journal of Cellular and Molecular Medicine*, 26(1), 88–98. https://doi.org/10.1111/jcmm.17034

Wang, M., Monticone, R. E., & McGraw, K. R. (2020). Proinflammation, profibrosis, and arterial aging. *Aging Medicine*, 3(3), 159–168. https://doi.org/10.1002/agm2.12099

Zhang, W., Chen, X., Huang, L., Lu, N., Zhou, L., Wu, G., & Chen, Y. (2014). Severe sepsis: Low expression of the renin-angiotensin system is associated with poor prognosis. *Experimental and Therapeutic Medicine*, *7*(5), 1342–1348. https://doi.org/10.3892/etm.2014.1566

SUPPORTING INFORMATION

Additional supporting information can be found online in the Supporting Information section at the end of this article.